

The Morphologically Divided Redshift Distribution of Faint Galaxies

Myungshin Im ^{1,6}, Richard E. Griffiths ², Avi Naim ², Kavan U. Ratnatunga ², Nathan Roche ³,
Richard F. Green ⁴, & Vicki L. Sarajedini ⁵

ABSTRACT

We have constructed a morphologically divided redshift distribution of faint field galaxies using a statistically unbiased sample of 196 galaxies brighter than $I = 21.5$ for which detailed morphological information (from the Hubble Space Telescope) as well as ground-based spectroscopic redshifts are available. Galaxies are classified into 3 rough morphological types according to their visual appearance (E/S0s, Spirals, Sdm/dE/Irr/Pec's), and redshift distributions are constructed for each type. The most striking feature is the abundance of low to moderate redshift Sdm/dE/Irr/Pec's at $I < 19.5$. This confirms that the faint end slope of the luminosity function (LF) is steep ($\alpha < -1.4$) for these objects. We also find that Sdm/dE/Irr/Pec's are fairly abundant at moderate redshifts, and this can be explained by strong luminosity evolution. However, the normalization factor (or the number density) of the LF of Sdm/dE/Irr/Pec's is not much higher than that of the local LF of Sdm/dE/Irr/Pec's. Furthermore, as we go to fainter magnitudes, the abundance of moderate to high redshift Irr/Pec's increases considerably. This cannot be explained by strong luminosity evolution of the dwarf galaxy populations alone: these Irr/Pec's are probably the progenitors of present day ellipticals and spiral galaxies which are undergoing rapid star formation or merging with their neighbors. On the other hand, the redshift distributions of E/S0s and spirals are fairly consistent those expected from passive luminosity evolution, and are only in slight disagreement with the non-evolving model.

Subject headings: cosmology: observations - galaxies: evolution - galaxies: luminosity function, mass function

Submitted to ApJ, Aug. 4th, 1997, Accepted July 27th, 1998

¹ Space Telescope Science Institute, Baltimore, MD 21218

² Dept. of Physics, Carnegie Mellon University, Pittsburgh, PA 15206

³ Dept. of Physics & Astronomy, University of Cardiff, P.O. Box 918, Cardiff CF2 3YB, Wales

⁴ NOAO, Tucson, AZ 85726-6732

⁵ UCO/Lick Observatory, University of California, Santa Cruz, CA 95064

⁶ Current address, UCO/Lick Observatory, University of California, Santa Cruz, CA 95064

1. Introduction

The images of faint field galaxies taken with the Wide Field and Planetary Camera (WFPC2) on the Hubble Space Telescope (HST) have provided invaluable morphological information on these objects. Using HST images with exposure times of about a few hours, reliable classification into basic morphological categories is possible down to a magnitude limit of $I \lesssim 22$. The Hubble Deep Field (HDF) observation, which is the deepest HST image so far, pushes this limit a few magnitudes fainter (Williams et al. 1996; Abraham et al. 1996; Naim et al. 1997). Using these morphological classifications, it has been established with data from the HST Medium Deep Survey (MDS) and the HDF that the number counts at faint magnitudes are dominated by galaxies of irregular or peculiar appearance with small sizes (Im et al. 1995a, 1995b; Griffiths et al. 1994a, 1994b; Casertano et al. 1995; Driver et al. 1995; Glazebrook et al. 1995). Also, there is evidence that E/S0s and spiral galaxies have undergone passive Luminosity Evolution (LE) or have not evolved much since $z = 1$ (Im et al. 1996; Schade et al. 1997; Pahre et al. 1996; Bender et al. 1996).

Despite these important findings, it has not yet been shown decisively as to what these faint irregular galaxies really are. The number counts and size distributions can be fitted well by assuming a model with a steep faint end slope ($\alpha < -1.4$) for the LF of Sdm/Irr galaxies, and they could thus be irregular galaxies with intrinsically low luminosity (Im et al. 1995a; Driver et al. 1995; Glazebrook et al. 1995). But a considerable fraction (about 40 %) of faint Irr/Pec's show signs which can be interpreted as evidence for interaction, suggesting that they could be merging galaxies at moderate redshift (Driver et al. 1995). Although the small sizes of these faint galaxies suggest that they may not be high redshift L_* galaxies undergoing starburst activity (Im et al. 1995a; Roche et al. 1996), it is not clear whether they are starbursting dwarf galaxies, or passively evolving/starbursting sub L_* spirals or E/S0s at $z \lesssim 1$.

Fortunately, more spectroscopic redshifts (hereafter z_{spec}) are becoming available for galaxies observed by the HST, thus providing a fair sample of faint galaxies with morphological information as well as z_{spec} . As described in the next section, we have obtained about 120 redshifts for MDS galaxies brighter than $I = 21$. Ground-based follow-up spectroscopic

observations have also been made for the HDF and for other MDS samples (Cohen et al. 1996a, 1996b; Phillips et al. 1997; Lowenthal et al. 1997; Forbes et al. 1996; Koo et al. 1996). Also, other groups have obtained HST WFPC2 images of galaxies in their redshift surveys (Schade et al. 1995; Cowie et al. 1996), and these HST data are now available for archival study. The total number of faint galaxies with spectroscopic redshifts and HST morphology now approaches about 500, and the time is therefore ripe to construct the redshift distributions for the morphologically divided faint galaxy samples.

2. Data

Our HST data include the HST MDS (Griffiths et al. 1994a), the strip survey of Groth et al. (1994), the WFPC2 observations of three different CFRS fields (Schade et al. 1995), the WFPC2 observations of the Hawaii Deep field (Cowie et al. 1996) and the HDF itself. The detection limit for the fields with medium levels of exposure covers the range $I \simeq 24 \sim 25$, while the detection limit for the HDF goes as deep as $I \simeq 28$. For each object detected, the observed image is fitted with simple model profiles (point source, $r^{1/4}$ profile and exponential profile) using a 2-dimensional maximum likelihood technique (Ratnatunga et al. 1998a). The resulting I -magnitude used here is a model-fit total magnitude in the HST flight system using the F814W filter, and this is almost equal to the conventional Johnson I magnitude (Holtzman et al. 1995).

The morphologically classified galaxies are matched with the spectroscopic redshift samples from Lilly et al. (1995a), Koo et al. (1996), Forbes et al. (1996), Cohen et al. (1996b), Cowie et al. (1996) and our own spectroscopic observations of MDS galaxies. Our own redshifts were obtained at the KPNO 4 meter telescope using the technique of multi-object spectroscopy with the Cryocam. Galaxies were chosen primarily for their brightness. Our limiting magnitude for successfully measured redshifts was $I \simeq 21.0$. These spectra cover the wavelength range from 4000Å to 9000Å with a resolution of 12Å, and redshifts are based on emission or absorption features. Adding these data to a collation of published results, a total of 464 galaxies with spectroscopic redshifts are found with HST images for morphological classification. The authors (MI, AN, and NR) have classified these galaxies according to their morphological ap-

pearance, dividing them into three broad classes, i.e., E/S0s, Spirals, and Sdm/dE/Irr/Pec galaxies. The agreement level for this broad morphological classification is about 90% at $I < 21.5$. For the purposes of this classification we have also used their luminosity profiles as supplemental information to distinguish the dE population from the normal E/S0 population (see Im et al. 1995b). These dE's should be distinguished from galaxies which are unclassifiable as a result of their small sizes and faint magnitudes. We treat Sdm/dE/Irr/Pec galaxies as one galaxy type since their LFs have a steep faint end slope, although we also find it plausible to treat Sdm/dE's and Irr/Pec's as different galaxy types in our analysis (see section 4). Coordinates, magnitudes, redshifts, and morphological classifications of these galaxies will appear in a separate publication (Ratnatunga et al. 1998b).

3. Sample selection

Our total sample of 464 galaxies is thus made up of heterogeneous subsamples. In order to construct a redshift distribution and to compare it with the predictions of galaxy evolution models, it is important to understand the completeness of each subsample. We need to make a correction for the fact that spectra were not taken for all the galaxies in some fields. Consequently, the completeness of redshift measurements varied from field to field, and thus a correction should be made for this. We define a quantity called "redshift detection rate" for this correction. This quantity is defined as the number of galaxies with actual redshift measurements versus the number of galaxies with photometric information for a given magnitude interval. This quantity must be distinguished with "sampling rate" which is defined as the number of galaxies for which spectra are obtained over the number of galaxies with photometric information.

We divide our sample into two magnitude bins $17.5 < I < 19.5$ (with the MDS sample) and $19.5 < I < 21.5$ (without MDS sample) in order to eliminate biases which could affect the analysis. We find that there are 196 galaxies at $17.5 < I < 21.5$. LeFevre et al. (1995) discuss the completeness and the sampling rate of the CFRS galaxies: the CFRS sample is about 90 % complete down to $I \simeq 21.5$ (or $I_{AB} = 22$), and the sampling rate for redshift measurements is about 22 %. They also discuss potential biases resulting from spectral ranges, magnitudes, and surface bright-

ness, and find that their sample is not seriously biased by these quantities (Hammer et al. 1995). For the Hawaii Deep Field sample, Cowie et al. (1996) note that their sample is about 93 % complete down to the magnitude limit of $I = 21.5$. Their sampling rate is 100 % and thus the effect of color, surface brightness or morphological bias is expected to be negligible. Redshift measurements of HDF galaxies are nearly complete to $I=21.5$ thanks to the collective efforts of several follow-up ground-based spectroscopic programs. Redshifts of galaxies in the HDF flanking fields have not been measured nearly as completely as those in the deep field. The sampling rate is about 50 % down to $I=22$ for galaxies in the flanking fields. For the MDS sample, we find that the completeness level varies depending on the observing runs. However, we note that redshift measurements of galaxies in the MDS sample are nearly complete down to $I < 20$. Therefore, we believe that our heterogeneous galaxy sample is free of bias at $I < 20$ within the MDS sample and to $I < 21.5$ without the MDS sample. To show that our sample is not biased in terms of colors or sizes, we also present size-magnitude and color-magnitude diagrams. Figure 1 shows the size-magnitude diagram for 6 different subsamples (the results of three MDS spectroscopic follow-up runs separated by the year when the redshifts were taken; the Westphal-Groth strip; the Hawaii field; and the HDF follow-ups for the flanking fields). We also present the color-magnitude diagrams for samples where more than one color is available (Figure 2). If the sizes and colors of galaxies within a given magnitude range have a similar distribution to that of all the galaxies within the same magnitude range in that field (or fields), then those galaxies with redshifts are considered to have been randomly selected. Figures 1 and 2 show that there is no serious bias in terms of colors and sizes at the adopted magnitude limits.

As a quantitative measure of the possible bias in the redshift sample, we have also studied the V/V_{max} statistic for each galaxy type (Tables 1 - 3). Originally proposed by Schmidt (1968), this quantity has been applied to various redshift samples to check if there is a bias in the sample or to find any evidence for cosmological evolution (e.g., see DellaCeca et al. 1992; Lilly et al. 1995b). The basic idea is the following: first, the enclosed volume (V) is calculated. The volume V is defined as the volume between the point where each galaxy is located and the closest point from the observer where a galaxy with the same ab-

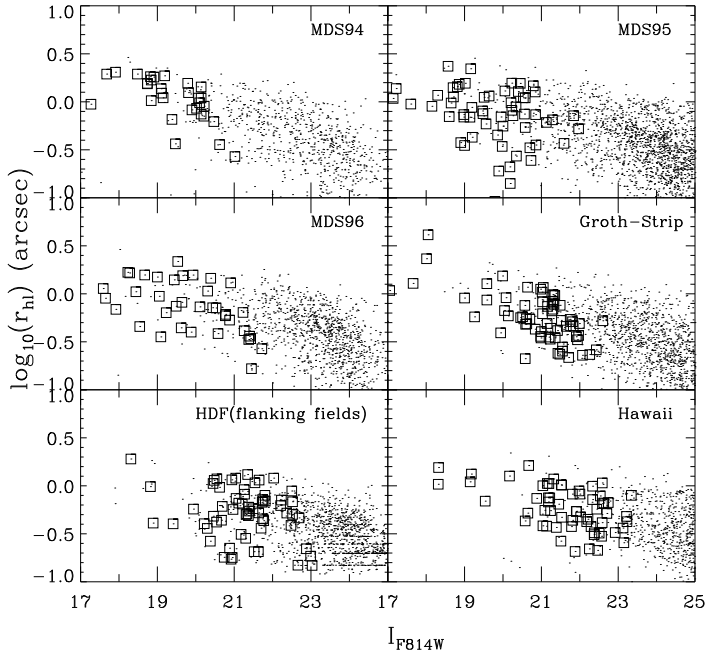


Fig.1: The size-magnitude relation of various redshift samples (squares) superposed on the relation for the total sample.

absolute magnitude could possibly be found within the observational selection window (magnitude limit and redshift limit). Then, the volume V is compared with the maximum volume (V_{max}) where the galaxy could be found within the observational selection window. If galaxies in the sample are randomly distributed in volume space, the quantity V/V_{max} s will have values randomly scattered between 0 to 1. Consequently, the mean value of V/V_{max} s for the randomly selected sample will be 0.5, and any deviation from it would suggest some kind of bias in the sample which could originate from either an evolutionary or observational selection effect. Mathematically, V/V_{max} is calculated using the following equations.

$$V = \int_{max(z_1, z_{m1})}^z (dV/dz) dz \quad (1)$$

$$V_{max} = \int_{max(z_L, z_{m1})}^{min(z_2, z_{m2})} (dV/dz) dz \quad (2)$$

where z_1 and z_2 are the lower or upper limits of the redshift interval, m_1 and m_2 are the lower or up-

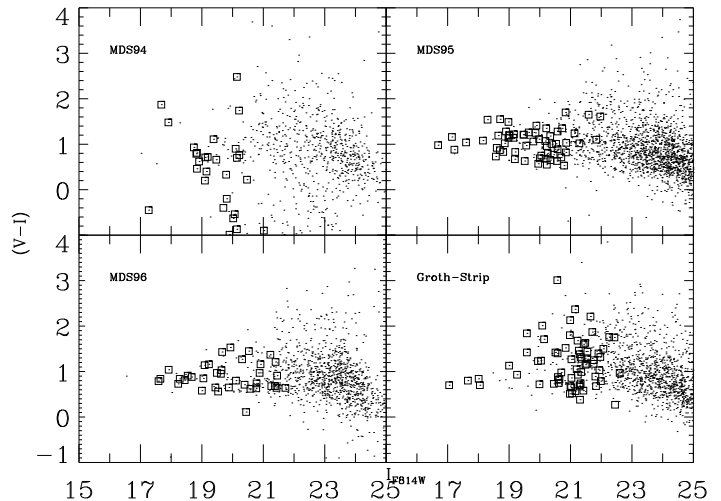


Fig.2: The color-magnitude relation of various redshift samples (squares) superposed on the relation for the total sample.

per limits of the magnitude interval, z_{m1} and z_{m2} are redshifts where the galaxy would be located if it has apparent magnitudes m_1 and m_2 respectively, and (dV/dz) is the volume element per unit redshift interval.

To obtain z_{m1} or z_{m2} , we need to estimate the absolute magnitude of each object and thus the (E+K) correction for each galaxy type needs to be understood. However, (E+K) corrections are not yet well known. Rather than using uncertain (E+K) corrections, we have used K-corrections to estimate the absolute magnitude of each galaxy. This could lead to an underestimate of V_{max} if there were luminosity evolution (i.e, the brightening of galaxies as a function of redshift). Hence, we would expect to get $\langle V/V_{max} \rangle > 0.5$ for a statistically unbiased sample of passively evolving galaxies. On the other hand, if our sample is biased against detection of high redshift galaxies, we expect to get $\langle V/V_{max} \rangle < 0.5$.

Tables 1, 2, and 3 show the values of $\langle V/V_{max} \rangle$ for different types of galaxies in different datasets and apparent magnitude ranges. The first number in parentheses is the actual number of galaxies with redshifts and the second number has been corrected for sampling (see the explanation below). All errors are $1-\sigma$, ignoring any effects of field to field fluctuations and small scale clustering. Thus, the real errors are expected to be somewhat larger than those quoted. Also note that we estimated $\langle V/V_{max} \rangle$ for

a redshift interval of $0 < z < 1$. Some caution must be taken in the interpretation of the $\langle V/V_{max} \rangle$ values. Several of the surveys used here are slightly incomplete even at this redshift and magnitude interval, and therefore $\langle V/V_{max} \rangle$ could be somewhat underestimated for some galaxy types. For example, Hammer et al. (1997) note that it is very likely that redshifts of faint early type galaxies at $z > 0.8$ are unidentified due to instrumental reasons. Also, note that the $\langle V/V_{max} \rangle$ values could fluctuate significantly depending on the choice of the redshift interval, when galaxies are distributed nonuniformly or spikily in redshift space like the E/S0s in Fig.4. Several caveats in the interpretation of $\langle V/V_{max} \rangle$ values are discussed in Im & Casertano (1998).

The $\langle V/V_{max} \rangle$ values for each galaxy type agree well with the expected value of 0.5 - 0.6 within the errors, a result which is consistent with luminosity evolution or no evolution. Within the fainter magnitude range ($19.5 < I < 21.5$), the $\langle V/V_{max} \rangle$ values appear to be greater than 0.5 for all galaxy types. When galaxies evolve passively without significant changes in their number density, we expect $\langle V/V_{max} \rangle \simeq 0.55$ if they are analysed assuming only k-corrections (see, for example Im et al. 1996). The $\langle V/V_{max} \rangle$ values of all types of galaxies agree well with this expectation. This would tend to support the model of pure luminosity evolution of galaxies at moderate to high redshift without strong number evolution, but this cannot be taken too seriously since the errors are not sufficiently small. Implications for galaxy evolution based upon the $\langle V/V_{max} \rangle$ values are discussed in more detail in the next section.

In the next step, we estimated the redshift detection rate as a function of apparent I magnitude. We defined the redshift detection rate to be the number of galaxies with redshift divided by the total number of galaxies in a given magnitude bin. Table 4 shows the redshift detection rate for the 7 subsamples as a function of I -band apparent magnitude. The redshift detection rate may vary as a function of magnitude even in the same subsample. To construct the redshift distribution, we used the inverse of the redshift detection rate to weight the number of galaxies with redshifts in a given magnitude bin.

4. Type-dependent redshift distribution

The redshift distribution of E/S0s, Spirals and Sdm/dE/Irr/Pec's are plotted as histograms in Fig.3

($17.5 < I < 19.5$) and Fig.4 ($19.5 < I < 21.5$). Thin and thick lines show the distributions before and after the application of the redshift detection rate correction. Errors based on poissonian statistics are shown for the thick lines. Along with the data, we have plotted the predicted redshift distribution using i) the no evolution (NE) model (dashed line) and ii) the passive LE model (solid line or dotted line). The parameters for the LF of each type of galaxy are listed in Table 5. Especially for the Sdm/dE/Irr/Pec's, two LE models are used according to the faint end slope of the LF, one for $\alpha = -1.87$ (solid line) and one for $\alpha = -1.5$ (dotted line). At $17.5 < I < 19.5$, we used all the subsamples in Table 2, since they all have magnitude limits fainter than $I = 19.5$. The most remarkable feature in Fig. 3 is the abundance of Sdm/dE/Irr/Pec galaxies at low redshift. The redshift distribution for these galaxies peaks at $z \lesssim 0.1$, and it is very difficult to obtain this kind of redshift distribution without adopting a LF with a steep faint end slope, confirming previous suspicions (Marzke et al. 1994; Gronwall & Koo 1995; Im et al. 1995b). In particular, we find that the number of these Sdm/dE/Irr/Pec's is consistent with the prediction from the LF of Marzke et al. (1994) within a factor of a few. Further, the redshift distribution of Sdm/dE/Irr/Pec's can be fit by assuming strong LE. We have used the LE model described by Driver et al. (1996). For the luminosity evolution parameter, we used $\beta = 0.7$. The existence of the $z \simeq 0.3 \sim 0.5$ Sdm/dE/Irr/Pec's is easy to understand in the context of strong LE. A similar conclusion has been reached from a 5-color survey of faint galaxies (Liu et al. 1997). In contrast, the redshift distributions of E/S0s and spirals are consistent with the predictions of the passive LE model as well as those of the NE model.

At $19.5 < I < 21.5$, a different picture emerges for the Sdm/dE/Irr/Pec galaxies. The MDS sample is excluded from the analysis in this magnitude interval since the magnitude limit of the MDS sample is $I \simeq 20$. No significant difference is found between the E/S0, spiral, and Sdm/dE/Irr/Pec redshift distributions, contrary to the prediction of dwarf-rich NE models where we would expect to find the peak of the redshift distribution to be at $z \simeq 0.1$ (dashed line). The LE model also fails to match the observed redshift distribution (solid line). When the faint end slope of the LF is reduced to $\alpha = -1.5$ (dotted line, model II), the overall shape of the redshift distribution can be matched better except for the normaliza-

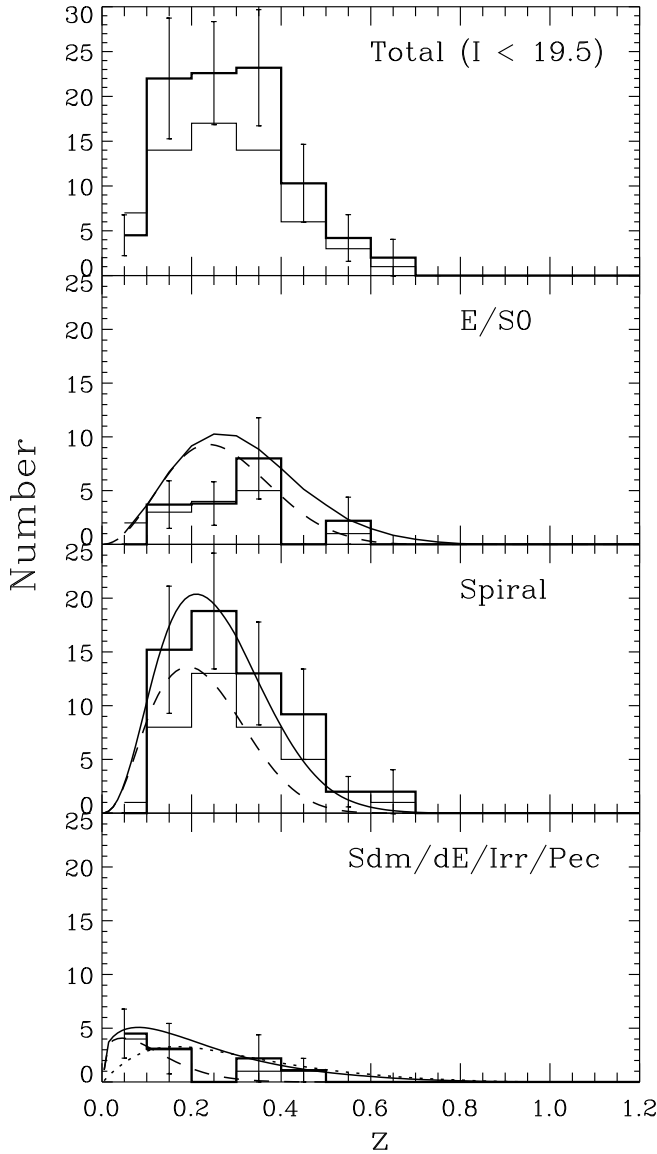


Fig.3: The morphologically divided redshift distribution of galaxies at $I < 19.5$. The solid histogram shows the distribution after the redshift detection rate correction is applied. The predicted distribution from passive LE models are represented by the solid line and the dotted line (model II for Sdm/dE/Irr/Pec), and the dashed line is for the NE model (see section 4). The total number of galaxies used for this graph is 62, and the number of fields is 54.

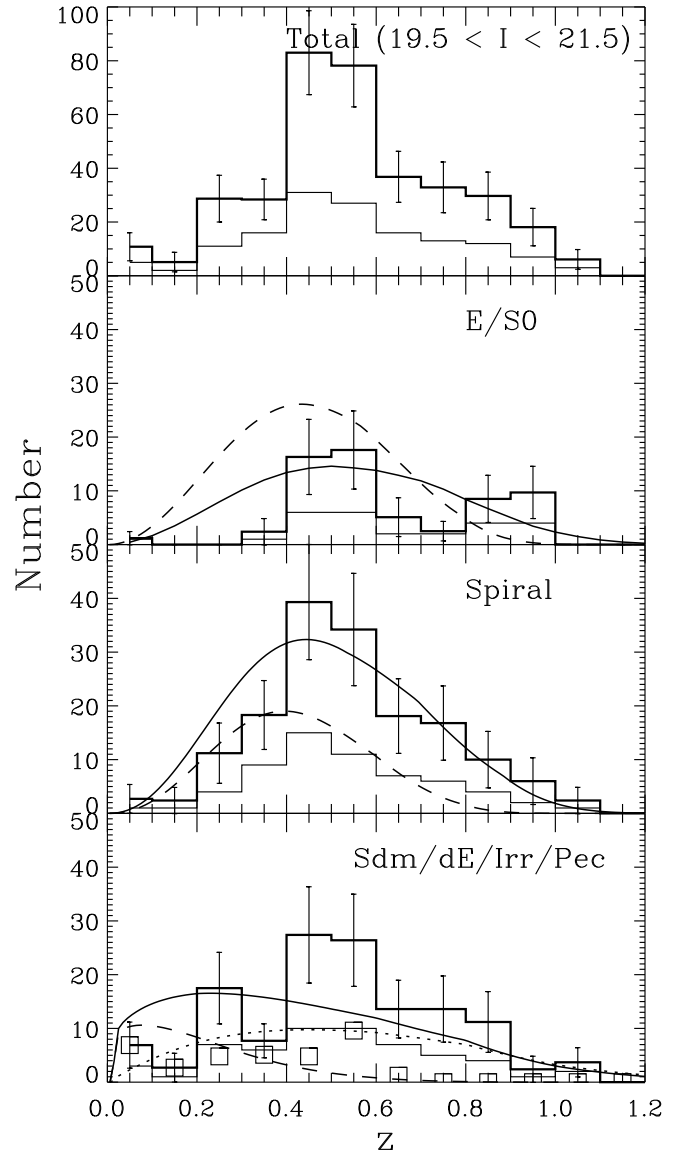


Fig.4: The morphologically divided redshift distribution of galaxies at $19.5 < I < 21.5$. The meaning of the lines is the same as Fig.3 except that the squares show the redshift distribution of Sdm/dE only with the redshift detection rate correction. The total number of galaxies used for this graph is 143, and the number of fields is 24.

tion. However, if we force the normalization to fit, we predict too many Sdm/dE/Irr/Pec's at the brighter magnitudes.

These results imply that: i) the Sdm/dE/Irr/Pec population cannot be described by a simple LE or NE model with a steep faint end slope for the LF, and that their evolution was much more complex; or that ii) the majority of apparently Sdm/dE/Irr/Pec galaxies are star-forming or interacting normal spirals or ellipticals, while some of the galaxies classified as Sdm/dE/Irr/Pec are actually accounted for by a simple dwarf rich LE model which occupy the low redshift domain of the distribution. To investigate hypothesis ii), we divided the Sdm/dE/Irr/Pec galaxies into two different populations, one which contains smooth objects (Sdm/dE) and the other which are not smooth (Irr/Pec). The redshift distribution of the smooth population is marked with rectangles in Fig.4. The smooth population accounts for the majority of the low redshift sample, while the non-smooth population is responsible for all the high redshift Sdm/dE/Irr/Pec objects ($z > 0.6$). Thus, most of the moderate to high redshift Sdm/dE/Irr/Pec's must be objects which are experiencing violent activity such as starbursts or merging. Verification of hypothesis i) is not a trivial task. As a simple prescription, we model the number evolution of Sdm/dE/Irr/Pec's as being proportional to $(1+z)^m$. Since the predicted numbers of Sdm/dE/Irr/Pec's are low by a factor of 2 - 3 at $z > 0.4$, it will be sufficient to adopt number evolution rising as $(1+z)^{2\sim 3}$ in order to fit the observed distribution.

The $\langle V/V_{max} \rangle$ value could, in principle, be a sensitive indicator of number evolution. However, since errors are not sufficiently small, the $\langle V/V_{max} \rangle$ values are consistent with both ~ 0.55 (strong luminosity evolution only) and ~ 0.6 (strong luminosity evolution plus number density evolution). Based on this test, it is difficult to judge which hypothesis is right.

The question still remains as to the nature of these moderate to high redshift Irr/Pec's: are they L_* - $sub L_*$ spirals that are forming stars more actively than the present day spirals, or are they the present-day dwarf galaxies which were in a starburst stage (Babul & Ferguson 1996) and disappeared later? To arrive at a full answer, other observables will be helpful, such as colors, sizes and velocity dispersions. A detailed analysis of colors, sizes and redshifts of these galaxies has been conducted by Roche et al. (1998).

The indications from this analysis are such that the colors of the Irr/Pec's show a wide dispersion on the color-redshift diagram indicating that some of these galaxies are more consistent with being spirals or E/S0s. Furthermore, the size-luminosity relation of Irr/Pec's at different redshifts indicates that simple LE is not enough to explain their compactness, and that strong LE or size evolution is necessary for some Irr/Pec's. There is also evidence for the existence of starbursting L_* - $sub L_*$ galaxies at $z \gtrsim 0.3$ from a 5-color photometric survey of faint galaxies (Liu et al. 1997). These pieces of evidence appear to favor hypothesis (ii), so that strong number evolution of the Irr/Pec population is not necessary.

Finally, we note that the redshift distributions of E/S0s and spiral galaxies at $19.5 < I < 21.5$ are consistent with the prediction of the passive LE model and the NE model. The NE models appear to fail to predict the right abundance of E/S0s and spirals at $z < 0.7$, but the difference may not be significant due to the uncertainty in the normalization of their LFs. A notable feature is the spiky nature of the distribution of E/S0s. This is expected since E/S0s are more clustered than other types of galaxies (e.g, Neuschaefer et al. 1997).

The $\langle V/V_{max} \rangle$ values of E/S0s and spirals are consistent with values greater than 0.5, supporting the idea that these galaxies evolved passively. In particular, our $\langle V/V_{max} \rangle$ value for E/S0 galaxies is significantly greater than 0.4 at $19.5 < I < 21.5$. This contradicts the result of Kauffmann et al. (1996) in which they reported a strong number evolution of early type galaxies at $z < 1$ ($\sim (1+z)^{-1.5}$). Their claim is based on the measurement of $\langle V/V_{max} \rangle \simeq 0.4$ for their color-selected early type galaxies. Our result from the morphologically selected E/S0 sample does not support such strong number evolution, confirming instead the earlier result from a much larger sample of morphologically selected E/S0s with photometric redshifts (Im et al. 1996) where we reported $\langle V/V_{max} \rangle \simeq 0.55 - 0.58$. This indicates that the number density of E/S0s has not changed significantly since $z=1$ (also see, Totani & Yoshii 1998; Im & Casertano 1998).

5. Conclusions

We have constructed morphologically divided redshift distributions of ~ 200 galaxies in two magnitude intervals, $I < 19$, and $19.5 < I < 21.5$. Redshifts of

these galaxies are taken from (largely published) spectroscopic observations and the morphological classification has been done using HST data. The observed redshift distribution of Sdm/dE/Irr/Pec's at $I < 19.5$ indicates that a very high normalization for the LF of Sdm/dE/Irr/Pec's is *unnecessary*, but the LF does need to have a steep faint end slope, confirming the findings from catalogs of nearby galaxies (Marzke et al. 1995). We also find that there was strong luminosity evolution for Sdm/dE/Irr/Pec's, but that the strong LE of Sdm/dE/Irr/Pec's alone is not enough to explain the moderate to high redshift Irr/Pec's at $I > 19.5$. Many Irr/Pec's at moderate to high redshift must be either starbursting spirals and E/S0s or disappearing dwarfs with a number density evolution of $\sim (1+z)^2$. The preliminary analysis of colors, sizes and redshifts of these galaxies indicates that many Irr/Pec's are likely to be sub L_* galaxies rather than starbursting dwarf galaxies. In contrast with this situation for Irr/Pec's, we find that the observed redshift distributions of E/S0s and spirals are consistent with the various evolutionary models, and do not require strong number density evolution at $z < 1$.

We thank an anonymous referee for useful comments and a careful review of the paper, and Pete Stockman for supporting this work. This paper is based on observations with the NASA/ESA Hubble Space Telescope, obtained at the Space Telescope Science Institute, which is operated by the Association of Universities for Research in Astronomy, Inc., under NASA contract NAS5-26555. The HST Medium Deep Survey has been funded by STScI grants GO2684 *et seq.* Also, this work is partly supported by the STScI Director's Discretionary Research Fund.

REFERENCES

- Abraham, R. G. et al. 1996, MNRAS, 279L, 47
- Babul, A., & Ferguson, H. C. 1996, 458, 100
- Bender, R., Ziegler, B., & Bruzual, G. 1996, ApJ, 463, 51L
- Bruzual A., G. & Charlot, S. 1996, ApJ, in preparation
- Casertano, S., Ratnatunga, K. U., Griffiths, R. E., Im, M., Neuschaefer, L. W., Ostrander, E. J., & Windhorst, R. A. 1995, ApJ, 453, 559
- Cohen, J. G., et al. 1996b, ApJ, 471, 5L
- Cohen, J. G., Hogg, D. W., Pahre, M. A., & Blanford, R. 1996a, ApJ, 462, 9L
- Cowie, L. L., Songaila, A., Hu, E. M., & Cohen, J. G. 1996, AJ, 112, 839
- Della Ceca, Roberto, et al. 1992, ApJ, 389, 491
- Driver, S. P., et al. 1996, ApJ, 466, 5L
- Driver, S. P., Windhorst, R. A., & Griffiths, R. E. 1995, ApJ, 453, 48
- Forbes, D. A., Phillips, A. C., Koo, D. C., & Illingworth, G. D. 1996, ApJ, 462, 89
- Glazebrook, K., Ellis, R. S., Santiago, B., & Griffiths, R. E. 1995, MNRAS, 275, L19
- Griffiths, R. E., et al., 1994a, ApJ, 437, 67
- Griffiths, R. E., et al., 1994b, ApJ, 435, L19
- Gronwall, C., & Koo, D. C. 1995, ApJ, 440, 1L
- Groth, E. J., et al. 1994, BAAS, 185, 5309
- Hammer, F., Crampton, D., LeFevre, O., & Lilly, S. J. 1995, ApJ455, 88
- Hammer, F., et al. 1997, ApJ, 481, 49
- Holtzman et al. 1995, PASP, 107, 1065
- Im, M., & Casertano, S. 1998, ApJsubmitted.
- Im, M., Casertano, S., Griffiths, R. E., Ratnatunga, K. U., & Tyson, J. A., 1995a, ApJ, 441, 494
- Im, M., Ratnatunga, K. U., Griffiths, R. E., Casertano, S. 1995b, ApJ, 445, L15
- Im, M., Griffiths, R. E., Ratnatunga, K. U., & Sarajedini, V. L. 1996 ApJ, 461, 79L
- Koo, D. C., et al. 1996, ApJ, 469, 535
- LeFevre, O., et al. 1995, ApJ, 455, 60
- Lilly, S. J., Tresse, L., Hammer, F., Crampton, D., & Le Fevre, O. 1995a, ApJ, 455, 108
- Lilly, S. J., Hammer, F., Le Fevre, O., & Crampton, D. 1995b, ApJ, 455, 75
- Liu, C. T., Green, R. F., Hall, P. B., & Osmer, P. S. 1997, ApJ, submitted.
- Lowenthal, J. D., et al. 1997, ApJ, 481, 673
- Marzke, R. O., Geller, M. J., Huchra, J. P., & Corwin, H. G., 1994, AJ, 108, 437
- Naim, A., Ratnatunga, K. U., & Griffiths, R. E. 1997, ApJ, 476, 510
- Neuschaefer, L. W., Im, M., Ratnatunga, K. U., Griffiths, R. E., & Casertano, S. 1997, ApJ, 480, 59
- Pahre, M. A., Djorgovski, S. G., & de Carvalho, R. R. 1996, ApJ, 456, 79L
- Phillips et al. 1997, ApJ, 489, 543
- Ratnatunga, K. U., et al. 1998a, ApJsubmitted
- Ratnatunga, K. U., et al. 1998b, in preparation
- Roche, N., Ratnatunga, K. U., Griffiths, R. E., Im, M., & Naim, A. 1998, MNRAS, 293, 157
- Roche, N., Ratnatunga, K. U., Griffiths, R. E., Im, M., & Neuschaefer, L. W. 1996, MNRAS, 282, 1247
- Schade, D., Barrientos, F. L., & Lopez-Cruz, O. 1997, ApJ, 477, 17L
- Schade, D. et al. 1995, ApJ, 451, 1L
- Schmidt, M. 1968, ApJ, 151, 393
- Totani, T., Yoshii, Y. 1998, ApJin press.
- Williams, R. E. et al. 1996, AJ, 112, 1335

TABLE 1
 $\langle V/V_{max} \rangle$ FOR EACH GALAXY TYPE

Galaxy	Magnitude Bin	
	17.5 < I < 19.5	19.5 < I < 21.5
Total	0.54 ± 0.04 (55,85)	0.55 ± 0.02 (141,355)
E/S0	0.40 ± 0.08 (13,17)	0.60 ± 0.05 (26,63)
Spirals	0.60 ± 0.05 (35,58)	0.53 ± 0.04 (61,162)
Sdm/dE/Im	0.59 ± 0.20 (2,3)	0.57 ± 0.07 (17,35)
Pec/Irr	0.38 ± 0.13 (5,7)	0.55 ± 0.05 (37,94)

TABLE 2
 $\langle V/V_{max} \rangle$ FOR EACH SURVEY (17.5 < I < 19.5)

Galaxy	Survey Name						
	MDS94	MDS95	MDS96	Lilly+Groth Strip	HDF	HDF(flanking)	Hawaii
Total	0.46 ± 0.08 (11,18)	0.59 ± 0.07 (15,21)	0.61 ± 0.09 (10,18)	0.46 ± 0.09 (9,15)	0.50 ± 0.14 (4,4)	0.78 ± 0.20 (2,4)	0.44 ± 0.14 (4,4)
E/S0	0.20 ± 0.14 (4,6)	0.38 ± 0.16 (3,3)	...	0.76 ± 0.20 (2,4)	0.47 ± 0.28 (1,1)	...	0.20 ± 0.20 (2,2)
Spirals	0.60 ± 0.11 (7,12)	0.65 ± 0.08 (11,17)	0.58 ± 0.09 (9,16)	0.30 ± 0.16 (3,5)	0.69 ± 0.20 (2,2)	0.78 ± 0.28 (1,4)	0.67 ± 0.20 (2,2)
Sdm/dE	0.83 ± 0.28 (1,2)	0.10 ± 0.28 (1,1)
Pec/Irr	...	0.35 ± 0.28 (1,1)	...	0.43 ± 0.16 (3,5)	0.16 ± 0.28 (1,1)

TABLE 3
 $\langle V/V_{max} \rangle$ FOR EACH SURVEY (19.5 < I < 21.5)

Galaxy	Survey Name			
	Lilly+Groth Strip	HDF	HDF(flanking)	Hawaii
Total	0.53 ± 0.03 (66,166)	0.59 ± 0.06 (24,51)	0.56 ± 0.05 (33,115)	0.58 ± 0.07 (18,23)
E/S0	0.60 ± 0.10 (8,20)	0.69 ± 0.10 (9,19)	0.54 ± 0.11 (6,21)	0.57 ± 0.16 (3,4)
Spirals	0.45 ± 0.05 (28,72)	0.62 ± 0.09 (10,24)	0.58 ± 0.07 (17,60)	0.58 ± 0.11 (6,7)
Sdm/dE	0.63 ± 0.10 (8,20)	0.04 ± 0.20 (2,2)	0.50 ± 0.20 (2,7)	0.63 ± 0.12 (5,6)
Pec/Irr	0.56 ± 0.06 (22,55)	0.39 ± 0.16 (3,6)	0.56 ± 0.10 (8,28)	0.54 ± 0.14 (4,5)

TABLE 4
REDSHIFT DETECTION RATES

I mag	MDS94	MDS95	MDS96	CFRS(+ GROTH strip)	Koo et al.	HDF	HDF(flanking)	Hawaii
17.5	1.00	1.00	0.68	1.00	...	1.00	0.00	1.00
18.5	0.71	0.90	0.68	0.33	0.68	...	0.43	1.00
19.5	0.47	0.49	0.56	0.26	0.00	1.00	0.25	1.00
20.5	0.23	0.31	0.28	0.32	0.20	0.94	0.30	0.71
21.5	0.00	0.04	0.12	0.39	0.12	0.80	0.28	0.71
22.5	0.00	0.00	0.00	0.03	0.05	0.41	0.06	0.34
23.5	0.00	0.00	0.00	0.00	0.00	0.05	0.00	...

TABLE 5
MODEL PARAMETERS

Galaxy type	α	$M_*(I) + 5 \log_{10}(h)$	$\phi_*(h^3 \text{ Mpc}^{-3})$	Star formation history
E/S0	-0.92	-21.5	0.005	1 Gyr burst, Salpeter IMF, & $z_{for} = 5$ (Bruzual & Charlot 1996)
Spirals	-0.92	-20.9	0.015	$\mu = 0.25$ (exponential), Scalo IMF, & $z_{for} = 3$ (Bruzual & Charlot 1996)
Sdm/dE/Irr/Pec (I)	-1.87	-19.6	0.004	Evolution model of Driver et al. (1996)
Sdm/dE/Irr/Pec (II)	-1.50	-19.6	0.004	Evolution model of Driver et al. (1996)